

Elastic carbon foam *via* direct carbonization of polymer foam for flexible electrodes and organic chemical absorption†

Cite this: DOI: 10.1039/c3ee41436a

Received 26th April 2013
Accepted 4th June 2013Shuiliang Chen,^{*ab} Guanghua He,^a Huan Hu,^a Shaoqin Jin,^a Yan Zhou,^a Yunyun He,^a Shuijian He,^a Feng Zhao^b and Haoqing Hou^{*a}

DOI: 10.1039/c3ee41436a

www.rsc.org/ees

Commonly, commercially available carbon foam derived from polymers shows brittle characteristics. In this paper, the concept of preparing an elastic carbon foam *via* the direct carbonization of a polymer foam is presented. A novel carbon foam with a 3D elastic interconnected network was prepared by the direct carbonization of melamine foam. The as-prepared carbon foam exhibited characteristics including excellent elasticity, extremely high porosity of over 99.6%, being lightweight with a density of 5 mg cm⁻³, a high specific surface area, tailored electrical conductivity, super-hydrophobicity and excellent absorptive properties towards oil and organic solvents. Two example applications as flexible electrodes and as an organic chemical absorbent have been demonstrated. For use as an electrode in supercapacitors, it could exhibit a specific capacitance of more than 250 F g⁻¹ in 1 M H₂SO₄ at a charge/discharge current density of 0.5 A g⁻¹. For use as an absorbent, it was able to absorb 148 to 411 times its own weight of organic solvents depending on the density of the solvents.

Carbon foam is a class of porous carbon materials with a three-dimensional (3D) interconnected network architecture and has been widely used in a wide range of fields,¹ such as electrodes in electrochemical cells,²⁻⁴ catalyst supports,^{5,6} heat insulators,⁷ electromagnetic shielding⁸ and oil removal.⁹ However, its brittle characteristics limit its applications, such as electrodes in flexible/portable devices. Recently, several carbon materials with 3D elastic/flexible interconnected networks have been developed as porous electrodes in flexible energy storage devices to meet various designs and needs to power modern portable equipment. These materials can mainly be classified into the following three types: (a) CNTs and graphene-coated polymer sponges,^{10,11} (b) 3D-CNTs and graphene networks, such

Broader context

Carbon foam is a three-dimensional (3D) porous carbon material with an interconnected network architecture. It is usually prepared by the carbonization/pyrolysis of foamed polymers. Recently, ultrathin and flexible energy storage devices have attracted much attention to meet various design and power needs of modern portable equipment. To build such devices, 3D flexible electrodes are required. Commonly, the commercially available carbon foams derived from polymers, *e.g.* reticulated vitreous carbon, show brittle characteristics. In this paper, we demonstrate the preparation of elastic carbon foam by the direct carbonization of a low density polymer foam, melamine foam. The elastic carbon foam not only could be used for flexible electrodes in supercapacitors, but also as an absorbent to remove waste organic chemicals and oils from water surfaces.

as CNT sponge¹² and graphene foam¹³ assembled by chemical vapor deposition (CVD), and (c) aerographite synthesized by a ZnO template CVD method.¹⁴ Although the former type has a 3D flexible and conductive interconnected network and shows excellent elasticity, the polymer skeleton limits their use under some harsh conditions, such as high temperature, and strong acid and base. The last two types would face the challenge of large-scale production due to their relatively high-cost and complex preparation processes.

Herein, we report a novel carbon foam with a 3D elastic interconnected network prepared by the direct carbonization of a polymer foam, which is denoted as an elastic carbon foam (ECF). Commonly, commercially available carbon foam derived from polymers, *e.g.* reticulated vitreous carbon (RVC), shows brittle characteristics.¹⁵ However, the carbon foam prepared in this paper shows characteristics of excellent elasticity, ultrahigh porosity of 99.6%, and being ultra lightweight with a low density of 5 mg cm⁻³, which is similar to the reported CNT sponge¹² and graphene foam.¹³ Moreover, it also shows hydrophobicity and excellent absorption properties towards a wide range of organic chemicals. In view of the unique 3D elastic interconnected carbon network and excellent characteristics, we will demonstrate the potential of the

^aDepartment of Chemistry and Chemical Engineering, Jiangxi Normal University, Nanchang, 330022, China. E-mail: slchen2006@yahoo.com.cn; haoqing@jxnu.edu.cn

^bInstitute of Urban Environment, Chinese Academy of Sciences, Xiamen, 361021, China

† Electronic supplementary information (ESI) available. See DOI: 10.1039/c3ee41436a

ECF for use as a flexible electrode and for the removal of waste organic chemicals and oil from water surfaces.

The precursor of the ECF is melamine foam (MF) which is a commercially available polymer foam. The main component of MF is formaldehyde–melamine resin (Fig. S1C, ESI†), which is an environmentally friendly material and is widely used in kitchen materials, *e.g.* utensils and plates, and in construction materials. MF shows an interconnected network architecture with a concave triangle fiber shape, as shown in Fig. S1, ESI†. It was first developed as an effective abrasive cleaner, and then was widely used as a soundproofing material. Generally, the commercial MFs have a low density in the range of 4–12 mg cm⁻³ and a high porosity of over 99%. The process for the preparation of the ECFs is very simple, only requiring direct carbonization of the MFs in an electric furnace under a nitrogen atmosphere at a temperature of over 800 °C. In this paper, MF with a density of 7.2 mg cm⁻³ is used as a raw material for the preparation of the ECF. As shown in Fig. 1A, a great shrinkage occurs during the carbonization process: a piece of MF with a white color and a size of 70 × 18 × 20 mm is converted to a black ECF with a size of about 46 × 10 × 13 mm. The great shrinkage is probably attributed to the low carbon yield of the MF precursor, which is calculated to be about 9%. SEM images in Fig. 1C and S1A, ESI† reveal that the as-prepared ECF inherits the interconnected network architecture and concave triangle fiber shape of the precursor MF.

The bulk ECF is extremely lightweight and elastic. For example, the ECF obtained by carbonizing MF at 1000 °C has an ultra-low density of about 5 mg cm⁻³ (due to the high porosity of ~99.6%), which is over ten times lower than that of the RVC (54 mg cm⁻³), and is comparable to the CNT-sponges

(5–10 mg cm⁻³)¹² and graphene foam (~5 mg cm⁻³).¹³ But unlike the RVC which shows a brittle characteristic, the ECF is elastic and can sustain a large-strain compressing or bending deformation, and recovers most of its volume elastically, as shown in Fig. 2 and Video 1 in the ESI.† As shown in Fig. 2A, uniaxial compression and rebound tests of four pieces of ECFs at different set strains (20–80%) display nearly reproducible results where all curves show an initial linear region at $\epsilon < 20\%$. Under moderate-strain compression ($\epsilon = 20$ to 60%), all the unloading curves are above the line $y = 0$ while returning to the original state, indicating a complete volume recovery without any plastic deformation. With a larger strain compression of 80%, it only shows a small plastic deformation of less than 5%. Compressing the ECF along different directions at the same strain of 50% reveals an anisotropic response in the stress–strain curves, but they all show excellent elasticity in the three orthogonal directions (Fig. 2B) and have a similar compressive strength of about 10 kPa. Moreover, Fig. S3, ESI† shows that the unloading curves of the ECFs prepared at temperatures of 700 to 1800 °C all are above the line $y = 0$, which demonstrates that the excellent elasticity of ECF is not limited by the preparation temperature.

After further investigation of the morphologies and the structure properties of the ECF and the RVC, it is proposed that the elasticity of the interconnected carbon architecture is related to the slenderness ratio (SR) of the interconnected carbon network. The SR is defined as \bar{L}_f/\bar{L}_{ss} , which is the ratio between the statistical average length of the fiber between the two junctions (\bar{L}_f) and the statistical average straight side length of the cross-sectioned regular triangle shape (\bar{L}_{ss}) in the foam materials, as illustrated in Fig. 1D. The as-prepared ECF with a density of 5 mg cm⁻³ has a high SR value of 26.7, nearly four times that of RVC (SR = 7.2). Like a chopstick, the higher the slenderness ratio (length/diameter), the better the flexibility. Likewise, the carbon foam materials with higher SR values show better flexibility. Thus, the ECF shows excellent elasticity but the RVC shows a brittle characteristic without any elasticity. Moreover, ECFs with different densities have been prepared and are listed in Table S1, ESI.† The samples of ECF-1 and ECF-2 with a \bar{L}_f/\bar{L}_{ss} of 16.6 and 11.5, generated 5.3% and 21.5% plastic deformations under compression, respectively. It also demonstrates that the higher SR leads to the lower flexibility.

The high SR of the ECF could be attributed to the low density (4–12 mg cm⁻³) and low carbon yield (~9%) of the precursor melamine foam, which results in the low density of up to 5 mg cm⁻³ and the ultra-high porosity of over 99% in the final ECFs. The low carbon yield of the MF is a result of the high content of the nitrogen element in the melamine resin, which is calculated to be about 50.9% according to the molecular formula in Fig. S1C, ESI† (C₆H₉N₆). Most of the nitrogen atoms are released as the gases N₂ and NH₃ during the carbonization process, and this leads to the formation of a large amount of micro and meso-pores (Fig. S6, ESI†). This causes a high specific surface area of 268 m² g⁻¹ in the ECF. For the conventional carbon precursors, phenolic resin¹⁶ and polyacrylonitrile,¹⁷ their carbon yields are generally over 50%, and the resulting carbon foams show brittle characteristics and low specific surface areas. Commercial polyurethane

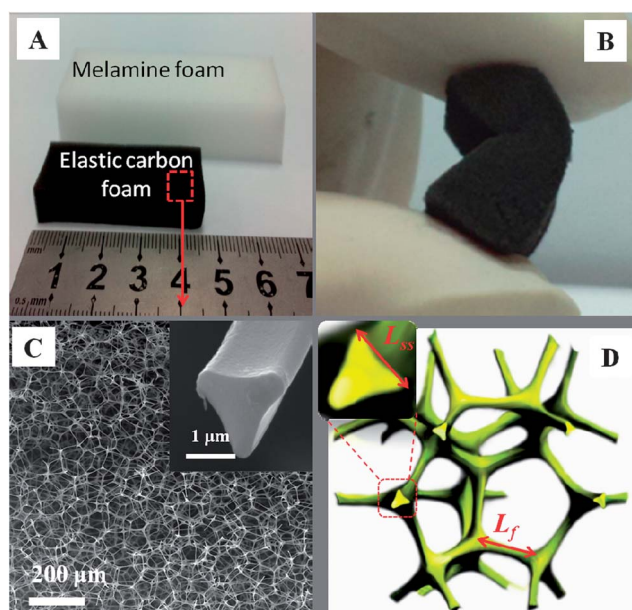


Fig. 1 Digital photos of (A) a piece of MF with a size of 70 × 18 × 20 mm and the derived ECF with a size of 46 × 10 × 13 mm and (B) ECF bent by finger tips. (C) Scanning electron microscopy image of ECF, inset is the cross-sectional image of one network fiber in the ECF, which shows a concave regular triangle shape. (D) Model for the ECF architecture.

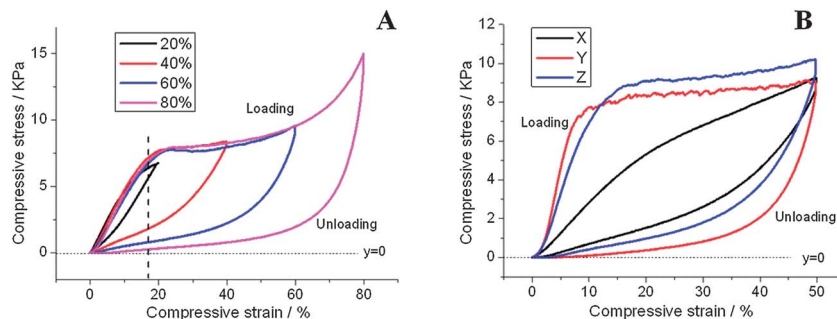


Fig. 2 (A) Loading and unloading compressive stress–strain curves of several ECFs at different set strains of 20%, 40%, 60%, and 80%, respectively. (B) Stress–strain curves recorded by compressing a cubic ECF along three orthogonal directions at compression strains of 50% (X: length, Y: width, Z: thickness).

foam has also been used to try to make a carbon foam, but its carbon yield is too low to make a carbon foam due to the existence of a large amount of oxygen in the molecular chains.

The electrical conductivity of the ECFs can be tailored for the applications of flexible electrodes, and as a support for active chemicals (or current collector) in electrochemical cells, *e.g.* flexible supercapacitors.^{18–20} The ECFs carbonized at 700, 800, 900, 1000 and 1800 °C show bulk electrical conductivities of 5.5×10^{-4} , 3.1×10^{-3} , 3.2×10^{-2} , 6.8×10^{-2} and 2.1 S cm^{-1} , respectively. The Raman spectroscopy of the ECFs (Fig. S4, ESI[†]) display that the intensity of the “G” peak (1593 cm^{-1}) increases with the increase in the carbonizing temperature, indicating an increase in the ordered graphitic layers in the ECFs. The electrochemical measurements reveal that the ECF displays an excellent capacitance performance. As shown in Fig. S5, ESI[†] taking the electrical conductivity and the specific capacitance into consideration, the ECF carbonized at 800 °C shows the best capacitive performance. It has a specific capacitance of more than 250 F g^{-1} in 1 M H_2SO_4 at a charge/discharge current density of 0.5 A g^{-1} . Moreover, it attains about 200 F g^{-1} at a higher current density of 10 A g^{-1} . The electrochemical stability of the ECF was tested at 50 A g^{-1} , and after 8000 cycles it still attained nearly 90% of its initial capacitance. The excellent capacitance performance of the ECF could be attributed to the following three aspects: (a) the high specific surface area derived from the meso- and micro-pores (Fig. S6, ESI[†]) leads to a high electrical double layer capacitance, (b) the presence of nitrogen with a content of more than 7.29% exists in pyridine-like and graphite-like states (Fig. S7, ESI[†]) and this contributes to the pseudocapacitance,³ and (c) the 3D interconnected carbon network architecture could ensure sufficient mass transportation under the high charge/discharge current density. Compared to the ECF prepared at 800 °C, the conductivity of the ECF prepared at a higher temperature, *e.g.* 1800 °C, increased by three orders of magnitude, and thus can be used as a current collector to support different active materials for a binder-free electrode in electrochemical cells. In view of the excellent elasticity and the tailored conductive properties, the ECFs show a great potential for the application as electrodes in flexible energy storage devices.

The ECF shows super-hydrophobicity and excellent absorptive properties towards a wide range of organic chemicals. As

shown in Fig. 3B and Video 2 in the ESI,[†] the ECF soaks up oil very quickly, but floats on the water surface. It demonstrates that the ECF can be used to remove waste oil from water. The ECF is also an excellent absorbent material for a wide range of organic liquids, such as ethanol, benzene, dimethylformamide, dimethylsulfoxide, ethylene glycol, hexane and chloroform. Fig. 3C and Video 3 in the ESI[†] display that the benzene film floating on the surface of the water is easily removed by the ECF. The absorption capacities (Q) of the ECF towards different organic solvents range from 148 to 411 times their own weight, with a larger Q for the higher density liquids, as summarized in Table 1. For chloroform, the absorption capacity of the ECF is 411 times, two times more than that reported for the CNTs sponge (about 180 times).¹² Moreover, as shown in Fig. 3A, the absorbed solvents in the ECF can be burnt in air without destroying its original 3D interconnected carbon architecture. The absorption/burning cyclic stability of the ECF was tested and the results are shown in Fig. S8, ESI[†]. The weight of the ECF decreased by about 50% after 10 absorption/burning cycles, indicating that a small amount of carbon is burnt off during the burning process. The absorbance (weight of the absorbed solvent) decreased, however, the Q of the ECF after 10 cycles

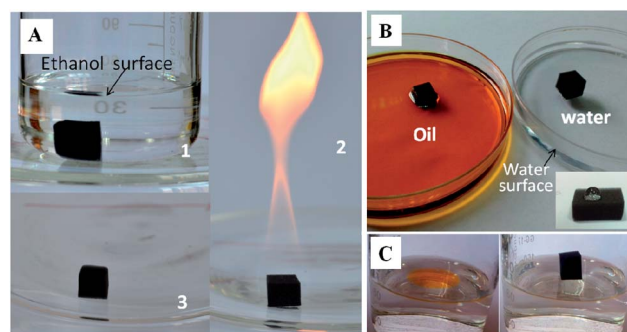


Fig. 3 (A) Digital images of (1) ECF with a size of $1 \times 1 \times 1.1 \text{ cm}^3$ immersed in ethanol, (2) burning of ethanol in the ECF, (3) after burning of ethanol from the ECF. It demonstrated that the ethanol can be directly and completely burned from the ECF without destroying the sponge-like structure. (B) ECF put in the oil and water. It reveals that the ECF possesses the properties of not oleophilicity but hydrophobicity. (C) Removal of benzene from the water surface using ECF: (left) a colored benzene film on the water surface, (right) the colored benzene film was absorbed by a piece of ECF.

Table 1 Absorption properties of the ECFs toward different solvents and oils

| Organic chemicals | Density of chemical (g cm ⁻³) | Absorption capacity (Q) ^a |
|-------------------|---|--------------------------------------|
| Ethanol | 0.791 | 148.4 |
| Dimethylformamide | 0.9445 | 261.2 |
| Dimethylsulfoxide | 1.10 | 273.5 |
| Ethylene glycol | 1.115 | 231.3 |
| Hexane | 0.6594 | 182.5 |
| Chloroform | 1.484 | 411.2 |
| Peanut oil | 0.92 | 257 |
| Vacuum pump oil | 0.88 | 188.6 |

^a Q: the ratio between the final and initial weight of carbon sponge after full absorption.

with ethanol did not decrease but showed a slight increase from 148 to 161 times.

In summary, the preparation of ECF by the direct carbonization of MF is demonstrated. The elasticity of the ECF is attributed to the high slenderness ratio which stems from the low density and low carbon yield of the MF precursor. Based on the novel elastic interconnected carbon network and the excellent characteristics of being lightweight, and having high porosity, super-hydrophobicity and excellent absorptive properties towards organic liquids, the novel ECF provides potential applications in the energy and environmental fields, such as for flexible electrodes, and the removal of waste organic chemicals and oil pollution from water surfaces. Moreover, the inexpensive raw materials of MF and the simple preparation process ensure that the large-scale production of the ECF is easy to be implemented.

Materials and methods

Preparation of ECFs

MFs were obtained from SINOYQX (Sichuan, China) and used as received. The MFs were put into an electric furnace and heated to a certain temperature (700, 800, 900, 1000 and 1800 °C) with a heating rate of 5 °C min⁻¹ under a nitrogen atmosphere and annealing for about 0.5 h at the final temperature to finish the carbonization process. The as-prepared ECFs were taken out after the temperature was cooled down to below 200 °C.

Characterization of ECFs

The morphologies of the MFs and ECFs were characterized by SEM (TESCAN vega 3, Czech Republic) and the carbon structure was analyzed by Raman spectroscopy (Lab Ram HR Jobin Yvon, French). The compressive and rebound mechanical tests were carried out by a mechanical tester CMT-8102 (SANS, Shenzhen, China) equipped with two flat-surface compression stages and a 100 N load cell. The ECFs for the mechanical tests were cut into cubic blocks with a size of (1 cm × 1 cm × 1 cm). The compressive and rebound speeds were controlled at 5 mm min⁻¹. The average straight side length of the cross-sectioned regular triangle shape (L_{ss}) and the average length of the fiber

between the two junctions (\bar{L}_f) in the ECFs were measured from SEM images of corresponding samples, in which at least one hundreds fibers were measured. The slenderness ratio (SR) is defined as \bar{L}_f/\bar{L}_{ss} . The electrical conductivity of the ECFs was measured by the standard four-point method using a four-probe conductivity measurement device (RST-8, Guangzhou, China). The element analysis of the ECF was conducted by using X-ray photoelectron spectroscopy (PHI Quantera). The specific surface area and the porous structure of the ECFs were measured by nitrogen sorption isotherm (Micromeritics Instrument Corp.).

Solvent and oil absorption of ECFs

The absorption capacities of the ECFs towards solvents and oils with different densities were measured, including ethanol, dimethylformamide, dimethylsulfoxide, ethylene glycol, hexane, chloroform, peanut oil and vacuum pump oil. The ECFs cut into a cubic shape were placed inside the solvents or oil for a set of time (e.g., 30 seconds) and then picked out. The weight of the ECFs before (m_0) and after (m) absorption were recorded for calculating the absorption capacity Q ($Q = m/m_0$).

Acknowledgements

We thank the SINOYQX for providing the melamine foam samples. This research was supported by the National Natural Science Foundation of China (grant no.: 51202096), the Science and Technology Project of Jiangxi Province (no. 20121BBE50024) and China Postdoctoral Science Foundation (no. 2012M520407).

References

- 1 J. Matos, E. B. Barros, J. M. Filho and A. G. S. Filho, *Handbook of Nanophysics: Functional Nanomaterials, Part II Nanoporous and Nanocage Materials*, ed. K. D. Sattler, CRC Press, 2010, p. 12.
- 2 L. Dimesso, C. Spanheimer, S. Jacke and W. Jaegermann, *J. Power Sources*, 2011, **196**, 6729–6734.
- 3 M. Kodama, J. Yamashita, Y. Soneda, H. Hatori and K. Kamegawa, *Carbon*, 2007, **45**, 1105–1107.
- 4 S. Chen, Q. Liu, G. He, Y. Zhou, H. Muddasir, X. Peng, S. Wang and H. Hou, *J. Mater. Chem.*, 2012, **22**, 18609–18613.
- 5 M. Wang, J. P. Ma, C. Chen, F. Lu, Z. T. Du, J. Y. Cai and J. Xu, *Chem. Commun.*, 2012, **48**, 10404–10406.
- 6 E. Kang, Y. S. Jung, A. S. Cavanagh, G. H. Kim, S. M. George, A. C. Dillon, J. K. Kim and J. Lee, *Adv. Funct. Mater.*, 2011, **21**, 2430–2438.
- 7 O. Mesalhy, K. Lafdi and A. Elgafy, *Carbon*, 2006, **44**, 2080–2088.
- 8 F. Moglie, D. Micheli, S. Laurenzi, M. Marchetti and V. M. Primiani, *Carbon*, 2012, **50**, 1972–1980.
- 9 X. C. Dong, J. Chen, Y. W. Ma, J. Wang, M. B. Chan-Park, X. M. Liu, L. H. Wang, W. Huang and P. Chen, *Chem. Commun.*, 2012, **48**, 10660–10662.

- 10 X. Xie, G. Yu, N. Liu, Z. Bao, C. S. Criddle and Y. Cui, *Energy Environ. Sci.*, 2012, **5**, 6862–6866.
- 11 X. Xie, M. Ye, L. Hu, N. Liu, J. R. McDonough, W. Chen, H. N. Alshareef, C. S. Criddle and Y. Cui, *Energy Environ. Sci.*, 2012, **5**, 5265–5270.
- 12 X. C. Gui, J. Q. Wei, K. L. Wang, A. Y. Cao, H. W. Zhu, Y. Jia, Q. K. Shu and D. H. Wu, *Adv. Mater.*, 2010, **22**, 617–621.
- 13 Z. Chen, W. Ren, L. Gao, B. Liu, S. Pei and H.-M. Cheng, *Nat. Mater.*, 2011, **10**, 424–428.
- 14 M. Mecklenburg, A. Schuchardt, Y. K. Mishra, S. Kaps, R. Adelung, A. Lotnyk, L. Kienle and K. Schulte, *Adv. Mater.*, 2012, **24**, 3486–3490.
- 15 M. Łukaszewski, A. Żurowski and A. Czerwiński, *J. Power Sources*, 2008, **185**, 1598–1604.
- 16 J. C. Lytle, J. M. Wallace, M. B. Sassin, A. J. Barrow, J. W. Long, J. L. Dysart, C. H. Renninger, M. P. Saunders, N. L. Brandell and D. R. Rolison, *Energy Environ. Sci.*, 2011, **4**, 1913–1925.
- 17 Y. Yang, F. Simeon, T. A. Hatton and G. C. Rutledge, *J. Appl. Polym. Sci.*, 2012, **124**, 3861–3870.
- 18 Y.-C. Chen, Y.-K. Hsu, Y.-G. Lin, Y.-K. Lin, Y.-Y. Horng, L.-C. Chen and K.-H. Chen, *Electrochim. Acta*, 2011, **56**, 7124–7130.
- 19 L. Hu, W. Chen, X. Xie, N. Liu, Y. Yang, H. Wu, Y. Yao, M. Pasta, H. N. Alshareef and Y. Cui, *ACS Nano*, 2011, **5**, 8904–8913.
- 20 L. Yuan, X.-H. Lu, X. Xiao, T. Zhai, J. Dai, F. Zhang, B. Hu, X. Wang, L. Gong, J. Chen, C. Hu, Y. Tong, J. Zhou and Z. L. Wang, *ACS Nano*, 2011, **6**, 656–661.